

Analysis of the Performance of mc-Si and CdTe Modules under Soiling Conditions

Pablo Ferrada¹[\[https://orcid.org/0000-0001-8260-5289\]](https://orcid.org/0000-0001-8260-5289), Martha Isabel Llaguno², Aitor Marzo³[\[https://orcid.org/0000-0001-7795-5241\]](https://orcid.org/0000-0001-7795-5241), and Gabriel Lopez⁴[\[https://orcid.org/0000-0003-0117-6713\]](https://orcid.org/0000-0003-0117-6713)

¹ Centro de Desarrollo Energético Antofagasta, Universidad de Antofagasta, Chile

² Universidad Autónoma de Zacatecas, Zacatecas, Mexico

³ Departamento de Óptica, Universidad de Granada, Spain

⁴ Departamento de Ingeniería Eléctrica y Térmica, de Diseño y Proyectos, Universidad de Huelva, Spain

Abstract. In this work, we study the soiling impact on the performance of two PV technologies installed in the south of Spain. For this purpose, we include electrical measurements as well as spectral aspects such as dust transmittance, quantum efficiency and the local solar spectrum to analyse their response. The studied technologies were multicrystalline silicon (mc-Si) and cadmium telluride (CdTe) PV modules. The solar spectra representative for clear sky, clean glass cover and soiled glass as well as the spectral response of the PV modules were used for the calculation of the photogenerated current density and spectral mismatch factor. Two cloudless days were chosen for analysis. In terms of the solar resource, these days did not exhibit large differences. Nevertheless, soiling was present to a different extent. When comparing the corresponding power output of the technologies on day 1 and day 2, the power losses at 12 UTC were 3 times larger for mc-Si and nearly the same for CdTe. This result shows that the soiling impacts differently on PV modules having different spectral responses.

Keywords: Solar Spectral Irradiance, Soiling, Spectral Response, Spectral Dust Transmittance

1. Introduction

Today, a country's economic and industrial development must balance energy supply with increasingly restrictive environmental requirements. In this context, renewable energy sources emerge as a competitive alternative to conventional energy sources. In addition to exploiting their own unlimited resources, renewable energy technologies are better adapted to said restrictive environmental requirements [1]. The International Renewable Energy Agency (IRENA)[2] reports that wind and solar were the renewable energy technologies that grew the most between 2016 and 2020. The statistics show that their average additions to the electricity grid were 152 TWh and 118 TWh, respectively [3]. More specifically, 99.5% of the growth in solar technologies corresponds to photovoltaics (PV) and 0.5% to concentrated solar power (CSP). The cumulative PV electricity generation capacity in 2020 reached 831 TWh.

The sunbelt is the band around the Earth where the greatest amount of annual solar irradiation is received. It lies between the 40° N and 35° S parallels, between the two tropics. Andalusia, in the south of Spain, is part of the sunbelt. It receives the highest radiation within Europe with values in the order of 2000 kWh/m² for the annual global horizontal irradiation (GHl_a) leading to a potential for energy yields in the order of 1800 kWh/kWp, according to SolarGIS [4]. These numbers are comparable and not far from values obtained in other locations with high potential for solar technologies. These include the Atacama Desert with the

largest solar resource, where a GHI of 2500 kWh/m² and energy yield of 2200 kWh/kWp are possible to obtain [5].

PV generation depends on several factors, such as the amount of solar radiation available at the site, the configuration of the PV plant and the type of PV technology used, each with a different spectral response to solar radiation [6–8]. However, local environmental conditions, such as ambient temperature or soiling, also have an impact in the PV generation [9–11].

Soiling on the protective glass of the PV modules reflects and absorbs part of the incident solar radiation. It reduces the amount of solar radiation which can be used by the PV cells and thus their productivity. The way in which soiling affects the incident solar radiation depends on the amount of deposited soiling, the type of material and the wavelength of the incident radiation [12,13]. The cleaning of a large PV plant involves high costs related to the materials to be used and the human resource. Therefore, companies must adjust their operation and maintenance plans to the local conditions, to minimise the economic impact due to production losses as well as the costs associated with PV plant maintenance. Therefore, it is crucial to keep tracking the impact of soiling on PV technologies.

In this work, we studied multicrystalline silicon (mc-Si) and cadmium telluride (CdTe) PV modules, exhibiting different spectral responses. To this regard, the impact of the solar resource available for these technologies was addressed by determining the spectral transmittance of soiling deposited on the PV covers. For that, an innovative device unique worldwide was used [14].

The aim of this work is to analyze the soiling effects on the performance of mc-Si and CdTe PV modules installed in southern Spain and discuss the role of the solar spectrum available for the clean and soiled modules.

2. Experimental

The Solar Testing Laboratory used for this research is located at the La Rábida Campus of the Universidad de Huelva (UHU), Huelva in the south of Spain. Figure 1 shows the facilities available. The PV technologies monitored were multicrystalline silicon (mc-Si) from Yingli Solar and cadmium telluride (CdTe) from Solar Innova PV modules, respectively. The maximum power at standard testing conditions (STC) of these technologies are 265 Wp for mc-Si and 56 Wp for CdTe.



Figure 1. Overview of the Solar Testing Laboratory of the Universidad de Huelva.

Two pairs of modules (see Figure 2) were monitored at a tilt angle of 22° and south facing using an I-V tracer (model PV-KLA, manufactured by Ingenieurbüro Mencke & Tegtmeyer GmbH) to obtain the current-voltage curves every five minutes. One PV module of each pair was cleaned two times a week, whereas the other ones were soiled naturally. Temperature sensors were placed at the back side of each module. A Si reference photocell (model Si-V-10TC-T by Ingenieurbüro Mencke & Tegtmeyer GmbH) at the same plane of the array determined the broadband global tilted irradiance G_{β} .



Figure 2. Multicrystalline Si (left picture) and CdTe PV modules (right picture).

The spectral transmittance of soiling $\tau_{s\lambda}$ was obtained from the ratio between the spectral irradiance measured by a spectroradiometer behind a soiled glass and that measured by a spectroradiometer placed behind a clean glass every minute (Figure 3). Both the PV modules and the dirty glass were exposed to the same natural soiling. The spectroradiometers had the same tilt and azimuth angles as the PV modules. Finally, the spectral direct irradiance $G_{b\lambda}$ was also measured on one-minute base time resolution. These measures along with the methodology developed in [14] allowed the values of several atmospheric variables employed as inputs by the spectral radiative code SMARTS [15] to be derived and used to obtain the spectral global tilted irradiance $G_{\beta\lambda}$.



Figure 3. Spectroradiometers installed behind glasses for determining the spectral dust transmittance.

3. Calculations

The photogenerated current density J_{ph} was calculated using Eq. 1 [5,6], whereas the spectral mismatch factor SF was computed through Eq. 2 [16]. The SF was expressed in terms of the spectral global tilted irradiance $G_{\beta\lambda}$, the spectral response of the technology SR and the reference AM1.5G spectrum G_{ref} . The SR is related to EQE_{λ} through $SR = q \lambda EQE_{\lambda} / (h c)$.

$$J_{ph} = \frac{q}{h c} \int_{\lambda_1}^{\lambda_2} \tau_{\lambda} G_{\beta\lambda} EQE_{\lambda} \lambda d\lambda \quad (1)$$

$$SF = \frac{\int_0^{4\mu m} G_{\beta\lambda} SR d\lambda \int_0^{4\mu m} G_{ref} d\lambda}{\int_0^{4\mu m} G_{ref} SR d\lambda \int_0^{4\mu m} G_{\beta\lambda} d\lambda} \quad (2)$$

4. Results

Two cloudless days were selected for an analysis using the methodology here presented: August 17, 2021 (day 1) and August 17, 2022 (day 2). See Figure 4a for a comparison of the broadband solar irradiance (GHI for the global horizontal irradiance and GTI for the global tilted irradiance) received on day 1 and day 2. In terms of GHI and GTI the two selected days do not show large differences. Also, meteorological conditions are similar between each day, and temperature modules present similar values along the days. The two previous months to day 1 and day 2 were almost rainless, and the experimental devices were soiled but to a different degree/extent, depending mainly on the number of previous hazy days. Since the three instants considered here for both days present similar incoming spectral irradiances and the

same sun-PV modules geometries, the only factor leading to the different power production of PV modules is due to the soiling. The power losses at 12 UTC were 10.2% for the mc-Si and 2.2% for the CdTe modules on day 1, based on the experimental data from the I-V tracer. The same calculation on day 2 led to 3.1% and 3.4% power loss for the mc-Si and CdTe modules respectively. An overview of the soiling ratio (SR) is depicted in Figure 4b. The SR factor is noisy at the early and later times; while the SR keeps stable from 9 UTC to 17 UTC, reaching a local maximum near 12 UTC. Based on the SR data at 12 UTC, on day 1 the current was reduced by 20% for mc-Si and 7% for CdTe; whereas on day 2 the current dropped by 4% for both mc-Si and CdTe modules. These values agree with the analysis based in the power output (larger soiling impact on day 1 compared to day 2).

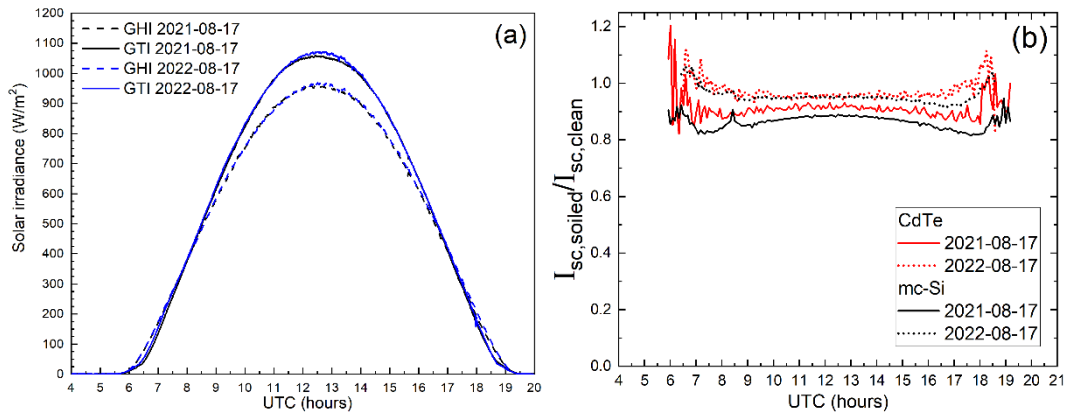


Figure 4. (a) Global horizontal (GHI) and global tilted (GTI) solar irradiance at day 1 and day 2. (b) Soiling ratio at day 1 and day 2 for mc-Si and CdTe modules.

The high variability presented on the soiling ratios of both PV technologies around the sunrise and sunset for both days could be related: i) to different dew condensing patterns on each PV module at the early hours of the morning, and ii) to moving shadows on the PV modules due to structure elements of the Laboratory at the end of the day. Nevertheless, a deeper analysis of these findings is out of the scope of this work.

The spectral transmittance of soiling corresponding at 8:00, 12:00 and 16:00 UTC are depicted in Figures 5a and 5b. It is noted soiling attenuates the incoming solar radiation according to the wavelength and the angle of the incident radiation (time). The global tilted spectral irradiance on day 1 and day 2 as well as the $E_{QE\lambda}$ corresponding to both technologies are shown in Figure 6a and 6b, respectively. The presented data in Figures 5 and 6 are used as input in Eq. 1 and 2.

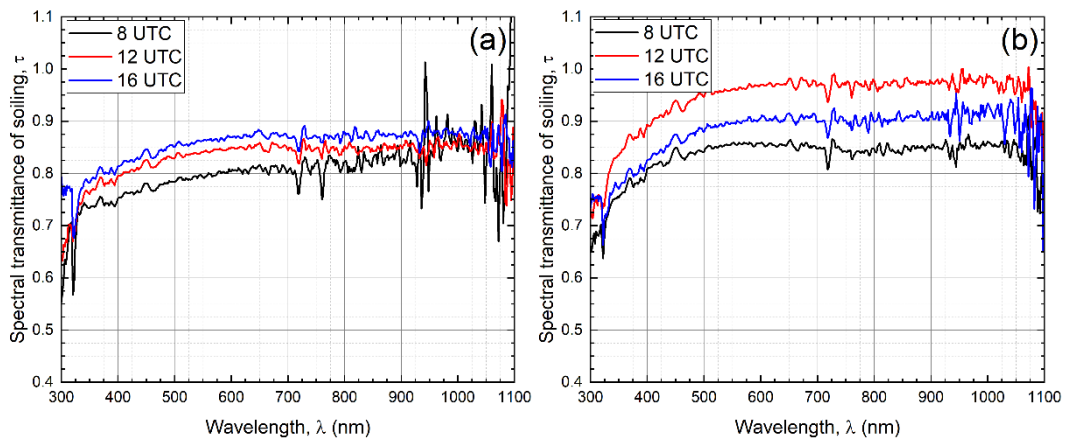


Figure 5. Spectral transmittance of soiling. (a) August 17, 2021. (b) August 17, 2022.

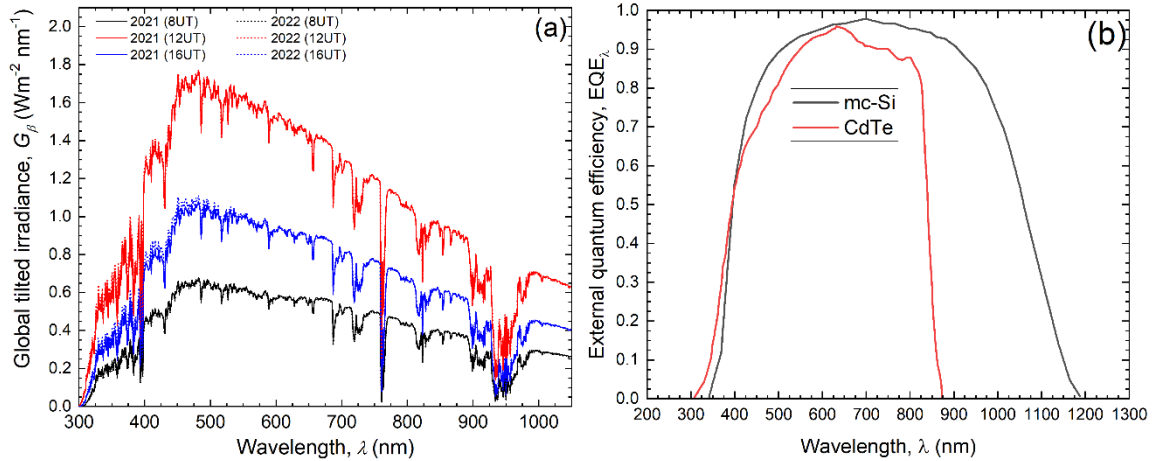


Figure 6. (a) Global tilted spectral irradiance on day 1 and day 2. (b) External quantum efficiency of mc-Si and CdTe modules.

Table 1 presents the J_{ph} values for the clean and soiled condition corresponding to the three instants selected on day 1. Likewise, Table 2 shows the J_{ph} values for the clean and soiled condition on day 2. The J_{ph} at STC is 36.65 mA/cm^2 for the mc-Si and 25 mA/cm^2 for the CdTe modules. The technologies exhibit similar J_{ph} losses when comparing the soiled and the clean condition. That is, 20%, 16% and 14% J_{ph} losses for both mc-Si and CdTe on day 1. This reduction is less pronounced on day 2, since the J_{ph} losses were up to 15%, 4% and 11% for both mc-Si and CdTe.

Table 1. J_{ph} for mc-Si and CdTe at clean and soiled condition on day 1.

UT (h)	G_{β} (W/m^2)	mc-Si modules		CdTe modules	
		$J_{ph,clean}$ (mA/cm^2)	$J_{ph,soiled}$ (mA/cm^2)	$J_{ph,clean}$ (mA/cm^2)	$J_{ph,soiled}$ (mA/cm^2)
8:00	152.8	14.0	11.4	10.1	8.1
12:00	1049	35.9	30.3	26.0	21.9
16:00	631.4	22.1	19.2	16.0	13.8

Table 2. J_{ph} for mc-Si and CdTe at clean and soiled condition on day 2.

UT (h)	G_{β} (W/m^2)	mc-Si modules		CdTe modules	
		$J_{ph,clean}$ (mA/cm^2)	$J_{ph,soiled}$ (mA/cm^2)	$J_{ph,clean}$ (mA/cm^2)	$J_{ph,soiled}$ (mA/cm^2)
8:00	156.7	13.9	11.8	10.0	8.5
12:00	1059	35.9	34.6	26.0	25.0
16:00	644.5	22.4	20.1	16.2	14.5

An analysis of the spectral mismatch factor (SF) at 12 UTC was performed. In an ideal case, the SF takes the value of 1. Thus, relative differences with respect to unity are described. The SF of mc-Si on day 1 (having a heavier soiling state compared to day 2) decreased 1.5% at clean and decreased 0.6% at soiled condition. Same calculations for CdTe resulted in an increase of 0.5% at clean and an increase of 1.1% at soiled conditions. The SF of mc-Si on day 2 (having a lighter soiling state compared to day 1) decreased 1.7% at clean and decreased

0.5% at soiled condition. Same calculations for CdTe resulted in an increase of 0.2% at clean and an increase of 1.1% at soiled conditions.

Table 3. SF for mc-Si and CdTe at clean and soiled condition on day 1.

UTC (h)	mc-Si modules		CdTe modules	
	SR_{clean}	SR_{soiled}	SR_{clean}	SR_{soiled}
8:00	0.99807	1.0098	1.0111	1.0099
12:00	0.98532	0.99441	1.0051	1.0113
16:00	0.99328	1.0022	1.0123	1.0179

Table 4. SF for mc-Si and CdTe at clean and soiled condition on day 2.

UTC (h)	mc-Si modules		CdTe modules	
	SR_{clean}	SR_{soiled}	SR_{clean}	SR_{soiled}
8:00	1.0003	1.007	1.0144	1.0199
12:00	0.98281	0.99511	1.0022	1.0108
16:00	0.98581	0.9978	1.0068	1.0142

5. Conclusions

The soiling impact on the PV modules performance has been analyzed taking its spectral dependence under outdoor conditions into account, thanks to the new experimental device developed in the Universidad de Huelva (Spain). The photogenerated current density (J_{ph}) and the spectral mismatch factor (SF) have been modified when soiling is present.

As expected, the J_{ph} of both technologies decreased at all times (8 UTC, 12 UTC and 16 UTC) on the two days analyzed under soiled conditions. The percentage reduction of J_{ph} for mc-Si and CdTe was nearly equal on day 1, being 20% at 8 UTC, 16% at 12 UTC and 14% at 16 UTC. On day 2, J_{ph} losses were less pronounced compared to day 1, where the reduction reached up to 15% for both technologies at 8 UTC, 3.6% for mc-Si and 4% for CdTe at 12 UTC and 11% for both technologies at 16 UTC. This larger impact of soiling on day 1 compared to day 2 agrees with the electrical measurements. For instance, the power losses at 12 UTC were 3.2 times larger for mc-Si and 0.7% times lesser for CdTe, when comparing their corresponding power output values on day 1 and day 2. This result proves that soiling impacts in different form on PV technologies with different spectral responses. Average values of soiling ratio obtained over a determined spectral band are thus not representative as using different PV technologies.

In terms of spectral mismatch factor, the mc-Si Crystalline silicon technology exhibited a SF value closer to 1 when it was soiled compared to the clean condition. This outcome occurred at different times and on the two days analyzed, existing at 12 UTC the largest difference between SF at soiled and SF at clean conditions. For the CdTe technology, this behavior is the opposite. The SF of clean modules was closer to 1 compared to SF at soiled condition.

Future works are focused to extend the present study to other atmospheric conditions. These results should be considered at the first stages of PV power plants design.

Data availability statement

The data that support the findings of this study are available on request.

Author contributions

Pablo Ferrada: Conceptualization, Methodology, Software, Validation, Formal Analysis, Investigation, Resources, Data Curation, Writing - Original Draft, Visualization.

Martha Isabel Llaguno: Writing - Review & Editing.

Aitor Marzo: Formal Analysis, Investigation, Data Curation, Writing – Review & Editing.

Gabriel Lopez: Conceptualization, Methodology, Software, Validation, Formal Analysis, Investigation, Resources, Data Curation, Writing - Review & Editing, Visualization, Supervision.

Competing interests

The authors declare that they have no competing interests.

Funding

Authors recognize the support provided in the context of following projects:

- ANID/FONDAP/15110019 funded by the Agencia Nacional de Investigación y Desarrollo (Chile).
- PVCastSOIL N° ENE2017-83790-C3-1-2-3-R funded by the Spanish Ministry of Economy, Industry, and Competitiveness, in collaboration with the European Regional Development Fund.
- RYC2021-031958-I, funded by the Spanish Ministerio de Ciencia e Innovación MCIN/AEI/10.13039/501100011033 and by the European Union "NextGenerationEU/PRTR".

References

1. M. Trigo-González, M. Cortés-Carmona, A. Marzo, J. Alonso-Montesinos, M. Martínez-Durbán, G. López, C. Portillo, F.J. Batlles, "Photovoltaic power electricity generation nowcasting combining sky camera images and learning supervised algorithms in the Southern Spain", *Renew. Energy*, 206, pp. 251–262, 2023. doi: 10.1016/J.RENENE.2023.01.111.
2. International Renewable Energy Agency, (2023). <https://www.irena.org> (accessed April 20, 2023).
3. Renewable Capacity Statistics 2021, International Renewable Energy Agency (IRENA), (2021).
4. Solar GIS: Global Horizontal Irradiation, (2022). <https://solargis.com/es/maps-and-gis-data/download/world> (accessed April 20, 2023).
5. P. Ferrada, A. Marzo, E. Cabrera, H. Chu, J. Rabanal, D. Diaz-Almeida, A. Schneider, R. Kopecek, "Potential for photogenerated current for silicon based photovoltaic modules in the Atacama Desert", *Sol. Energy* 144, pp. 580–593, 2017. doi:10.1016/j.solener.2017.01.053.
6. A. Marzo, P. Ferrada, F. Beiza, P. Besson, J. Alonso-Montesinos, J. Ballestrín, R. Román, C. Portillo, R. Escobar, E. Fuentealba, "Standard or local solar spectrum? Implications for solar technologies studies in the Atacama Desert", *Renew. Energy* 127, 2018. doi: 10.1016/j.renene.2018.05.039.
7. W. Jessen, S. Wilbert, C.A. Gueymard, J. Polo, Z. Bian, A. Driesse, A. Habte, A. Marzo, P.R. Armstrong, F. Vignola, L. Ramírez, "Proposal and evaluation of subordinate standard solar irradiance spectra for applications in solar energy systems", *Sol. Energy* 168, pp. 30–43, 2018, doi: 10.1016/J.SOLENER.2018.03.043.
8. P. Ferrada, A. Marzo, M.R. Ferrández, E.R. Reina, B. Ivorra, J. Correa-Puerta, V. del Campo, "Optimization of N-PERT Solar Cell under Atacama Desert Solar Spectrum", *Nanomaterials* 12, pp. 1-18, 2022, doi:10.3390/nano12203554.

9. J.F. Lelièvre, R. Couderc, N. Pinochet, L. Sicot, D. Munoz, R. Kopecek, P. Ferrada, A. Marzo, D. Olivares, F. Valencia, E. Urrejola, "Desert label development for improved reliability and durability of photovoltaic modules in harsh desert conditions", *Sol. Energy Mater. Sol. Cells.* 236, 111508, 2022. doi: 10.1016/j.solmat.2021.111508.
10. D. Olivares, A. Taquichiri, P. Ferrada, A. Marzo, M. Henríquez, D. Espinoza, E. Fuentealba, J. Llanos, "Soil Characterization and Soiling Impact to Facilitate Photovoltaic Installation", *Appl. Sci.* 12, pp. 1-12, 2022, doi:10.3390/app122010582.
11. B. Figgis, A. Nouviaire, Y. Wubulikasimu, W. Javed, B. Guo, A. Ait-Mokhtar, R. Belarbi, S. Ahzi, Y. Rémond, A. Ennaoui, "Investigation of factors affecting condensation on soiled PV modules", *Sol. Energy.* 159, pp. 488-500, 2018, doi: 10.1016/j.solener.2017.10.089.
12. D. Olivares, P. Ferrada, A. Marzo, J. Llanos, C. Miranda-Ostojic, V. del Campo, S. Bravo, E. Fuentealba, "Microstructural analysis of the PV module cementation process at the Solar Platform of the Atacama Desert", *Sol. Energy Mater. Sol. Cells.* 227, 111109, 2021, doi: 10.1016/j.solmat.2021.111109.
13. T. Sarver, A. Al-Qaraghuli, L.L. Kazmerski, "A comprehensive review of the impact of dust on the use of solar energy: History, investigations, results, literature, and mitigation approaches", *Renew. Sustain. Energy Rev.* 22, pp. 698–733, 2013. doi: 10.1016/j.rser.2012.12.065.
14. G. López, C.A. Gueymard, J. Polo, J. Alonso-Montesinos, A. Marzo, N. Martín-Chivelet, P. Ferrada, M.I. Escalona-Ilaguno, F.J. Batlles, "Increasing the Resolution and Spectral Range of Measured Direct Irradiance Spectra for PV Applications", *Remote Sens.* 15, 6, pp. 1-17, 2023. doi:10.3390/rs15061675.
15. C.A. Gueymard, "The SMARTS spectral irradiance model after 25 years: New developments and validation of reference spectra", *Sol. Energy.* 187, pp. 233–253, 2019, doi: 10.1016/j.solener.2019.05.048.
16. IEC 60904-7 (Ed. 4). Photovoltaic devices – Part 7: "Computation of the spectral mismatch correction for measurements of photovoltaic devices", 2019.